

## Status of TJ-II Flexible Helic Experiments and Issues Towards Steady State Operation

ALEJALDRE Carlos\*, ALONSO Javier, ALMOGUERA Luis, ASCASÍBAR Enrique, BACIERO Alfonso, BALBÍN Rosa, BLAUMOSER Martin, BOTIJA José, BRAÑAS Beatriz, DE LA CAL Eduardo, CAPPÀ Alvaro, CARRASCO Ricardo, CASTEJÓN Francisco, CEPERO Ramón José, CREMY Christopher, DONCEL José, EGUILIOR Sonsoles, ESTRADA Teresa, FERNÁNDEZ Angela, FUENTES Cándida, GARCÍA Angela, GARCÍA-CORTÉS Isabel, GUASP José, HERRANZ Jesús, HIDALGO Carlos, JIMÉNEZ Antonio Juan, KIRPITCHEV Igor, KRIVENSKI Vladimir, LABRADOR Ignacio, LAPAYESE Fernando, LIKIN Konstantine, LINIERS Macarena, LÓPEZ-FRAGUAS Antonio, LÓPEZ-SÁNCHEZ Antonio, DE LA LUNA Elena, MARTÍN Romualdo, MARTÍNEZ-LASO Luis, MEDRANO Mercedes, MÉNDEZ Purificación, MCCARTHY Kieran, MEDINA Francisco, VAN MILLIGEN Balduino, OCHANDO Marian, PACIOS Luis, PASTOR Ignacio, PEDROSA Angeles Maria, DE LA PEÑA Angel, PORTAS Ana, QIN Jiang, RODRÍGUEZ-RODRIGO Lina, SALAS Angel, SÁNCHEZ Edilberto, SÁNCHEZ Joaquín, TABARÉS Francisco, TAFALLA David, TRIBALDOS Victor, VEGA Jesús and ZURRO Bernardo

*Laboratorio Nacional de Fusión, Asociación EURATOM-CIEMAT, Madrid, Spain*

(Received: 19 January 2000 / Accepted: 24 July 2000)

### Abstract

The capability of the TJ-II Flexible Helic to obtain configurations with different magnetic parameters has been used in the last experimental campaign to introduce different rational values in the iota profile at several radial positions. Evidence of  $E \times B$  shear near some rationals has been observed pointing to some possible explanation for transport barrier formation. This issue is of utmost importance for so called “advanced” regimes in steady state plasmas. A description is also given of the last experiments conducted in TJ-II and their results.

### Keywords:

Stellarator, magnetic confinement, heliac, ECRH, transport

### 1. Introduction

TJ-II is a low magnetic shear stellarator of the Helic type with an average major radius of 1.5 m and an average minor radius of  $\leq 0.22$  m [1]. The magnetic field ( $B_0 \leq 1.2$  T) is generated by a system of poloidal, toroidal and vertical field coils. The central conductors, which provide the flexibility of the TJ-II device, consist of a circular coil and two helical coils which are wrapped around the central conductor. The main characteristics of TJ-II are the strong helical variation of its magnetic axis, the very favourable MHD

characteristics with potential for high beta operation and the capability to produce bean shaped plasmas with a wide range of operational flexibility (*i.e.*, its rotational transform and magnetic well depth can be varied over a wide range). Two gyrotrons (53.2 GHz, up to 700 kW total) have been installed for the first stage, in a second stage, 2 MW of additional NBI will be available. The existence of closed and nested magnetic surfaces, in good agreement with the calculated ones, has been demonstrated in TJ-II by means of magnetic surface

\*Corresponding author's e-mail: [carlos.alejaldre@ciemat.es](mailto:carlos.alejaldre@ciemat.es)

measurements carried out at low magnetic field [2].

Using TJ-II flexibility and a set of state of the art diagnostics, a configuration scan has been initiated which shows a significant modification in plasma profiles and stored energies in the device. Stored energy scales with  $\iota$  and plasma volume.

A particular and important issue for steady-state operation of so called "advance modes" in Tokamaks and to improve/optimize Stellarator performance is the understanding (and control) of transport barrier formation in these systems. In TJ-II, evidence of sheared  $E \times B$  flows associated with the presence of rational surfaces has been observed in the edge region of the stellarator together with an improvement of particle confinement of high energy electrons. This mechanism may be associated with the widely reported spontaneous formation of transport barriers at rational surfaces in magnetically confined plasmas.

## 2. Characteristics of The Heating System

Until now, heating has been performed in TJ-II using two 350 kW gyrotrons ( $f = 53.2$  GHz) with a pulse length up to 1 s which are coupled to the plasma by means of two quasi-optical transmission lines. The first quasi-optical transmission (QTL1) line allows perpendicular power injection while the second one (QTL2) is equipped with a movable mirror, located inside the vacuum chamber, that can be rotated both poloidally and toroidally. The power density at the resonance ranges from  $1 \text{ W/cm}^3$  for the QTL1 line to  $25 \text{ W/cm}^3$  for the QTL2 line. A power transmission efficiency of 0.9 has been achieved along the mirror lines and the wave beam diameter is  $\sim 10$  cm (QTL1) and  $\sim 2$  cm (QTL2) at the plasma border.

## 3. Wall Conditioning

After the vacuum vessel is baked at  $150^\circ\text{C}$ , (the total cycle lasting 30 h), a significant reduction of water is observed, as expected, leading to a decrease of the total base pressure, which achieved values in the order of  $5 \times 10^{-8}$  mbar. Only He glow discharge conditioning was used prior to the normal operation, in order to minimise the production of water during the conditioning at room temperature. The direct impact of the lower base pressure in machine operation can be basically reduced to a strong decrease of Hard X Ray emission during the rise of the currents, that leads to a better reproducibility of the plasma behaviour, and the suppression of gas desorption due to the direct impact of the highly focused microwave heating line (QTL2, up to

300 kW) on surfaces close to the plasma.

For low ( $\approx 150$  kW) or medium ( $\approx 350$  kW) ECRH power operation, the lowest possible density value was  $5 \times 10^{12} \text{ cm}^{-3}$ , due to He desorption from the walls, trapped during the overnight GD conditioning. As a consequence of the aforementioned plasma-wall coupling, this value used to rise over the cut-off when the second gyrotron was added to the plasma. In order to achieve a better control of the particle density under the 300–600 kW operation, a new conditioning protocol was adopted: a short (20 min) glow discharge in Ar was systematically used in order to remove the implanted He. The much lower probability of ion implantation in the metal of Ar ions precluded the significant contribution of that species to the hot plasmas, as witnessed by mass spectrometry. Therefore, density control was possible from the beginning of the operational day by this technique.

## 4. Plasma Profiles and Transport in ECRH Plasmas

Plasma discharges lasting up to 300 ms with central electron temperatures up to 1.5 keV, ion temperatures of 0.11 keV, plasma densities in the range  $(0.5\text{--}1.5) \times 10^{19} \text{ m}^{-3}$  and global energy confinement times up to 5 ms have been achieved using 100–600 kW of ECRH heating power. Confinement properties have been found to be strongly dependent on plasma configuration.

ECRH deposition profiles have an effect on temperature profiles and confinement times for different poloidal angles of the internal mirror of the QTL2 line. Thomson scattering and ECE system measurements show peaked temperature profiles in on-axis ECRH heated discharges while in off-axis heated discharges the central electron temperature and the energy confinement time decrease but rather flat density profiles in both on and off-axis heating, see fig. 1. In this experiment, the X ray flux (20–200 keV) decreases as the confinement time decreases. Non-Maxwellian features have been observed in electron distribution functions over the 1–5 keV energy range. Their possible link with ECRH induced deformation of the electron distribution is under investigation. The ECRH power density,  $1 \text{ W/cm}^3$  (QTL1 line) and  $25 \text{ W/cm}^3$  (QTL2 line), has an influence on the maximum central electron temperatures attainable.

The 1.5 D predictive transport code Proctr has been used to simulate TJ-II discharges. Electron heat conductivity is assumed to have a global dependence on electron density and temperature as in LHD scaling law and

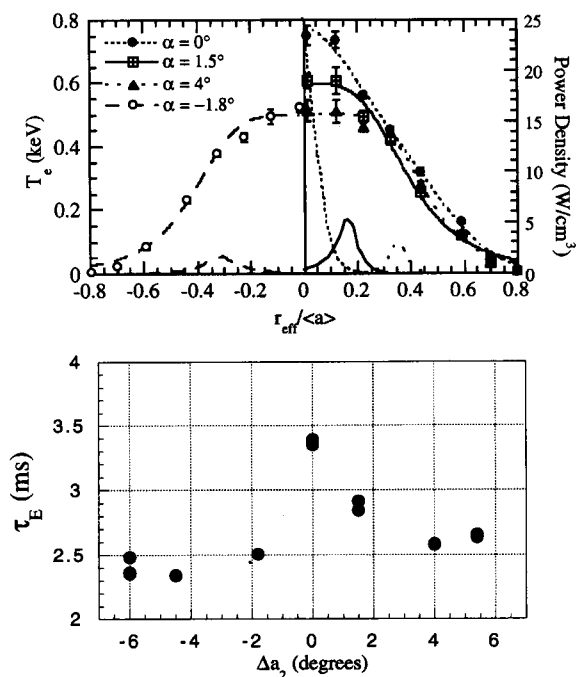


Fig. 1 The figure above shows the electron temperature profiles for on and off axis deposition of ECRH power at several launching angles together with the calculated deposition profiles. Below is the energy confinement time dependence with the launching angle.

is adjusted to give a temperature profile similar to the experimental one. Ion transport is simulated by neo-classical theory and impurity transport is also considered, being C and O the main plasma impurities used in the simulation with concentrations of several percents. Electron density flux is obtained from the fluxes densities of all the ions, assuming ambipolarity, and particle transport parameters are chosen to obtain a density profile similar to the experimental one. The heat conductivity obtained is about  $3 \text{ m}^2/\text{s}$  in the plasma core region and increases as the plasma boundary region is approached. Monte Carlo computations of neo-classical transport in the TJ-II stellarator have also been made and show that the expected neo-classical energy confinement time is about a factor of two larger than that measured experimentally. For typical TJ-II plasma conditions, i.e., the long mean free path collisionality regime, the ambipolar radial electric field is expected to be positive. This is in agreement with poloidal rotation measurements made in TJ-II which show that impurity ions (as determined from CV lines) rotate in the ion-diamagnetic drift direction and it is consistent with positive radial electric fields in the range of tens of V/m.

## 5. ECRH Modulation Experiments

ECRH modulation experiments have been performed in TJ-II with the goal of estimating the power deposition profile. The response of the modulation on ECE signals have been studied at both high field and low field sides. The HFS signals allow to study the influence of modulation in the thermal part of the distribution function and the outermost channels of LFS allow to consider the effect on superthermal electrons.

Experiments have been performed at four modulation frequencies: 10 kHz, 5 kHz, 1.5 kHz and 0.5 kHz. The high frequency modulation experiments have shown that only central channels react to the modulation of the power, while in the low frequency case outwards heat pulse propagation is observed. Power deposition profile is extracted directly from 10 kHz-modulation experiments by the fitting of the amplitude of Fourier Transform of ECE signals.

## 6. Configuration Effects: Rotational Transform and Rational Surfaces

Global confinement properties have been found to be strongly dependent on plasma configuration and preliminary could be said that follow better LHD scaling law than ISS95 due mainly to the iota dependence of the latter. The stored energy (W) increases as both the plasma volume ( $0.52\text{--}1.10 \text{ m}^3$ ) and the rotational transform (iota ( $a$ ) =  $1.32\text{--}1.73$ ) were modified. The optimal confinement has been found when major low order resonances are avoided. Interestingly,  $W/a^2$  increases with iota, thus suggesting improved stored energy with iota.

A magnetic configuration scan was done to move the  $4/3$  and  $8/5$  natural resonances from the edge to the central region of the plasma. The comparison between electron temperature profiles measured in plasma configurations with and without the  $4/3$  resonance inside the plasma shows that plasma profiles are significantly modified. Experimental values are in agreement with the expected width of the  $4/3$  resonance in the low shear TJ-II obtained from equilibrium calculations.

The natural  $8/5$  rational surface, as predicted by vacuum magnetic field calculations, has been observed as a flattening in the edge profiles in the plasma configuration with iota ( $a$ ) =  $1.6$  [3]. The flattening in density and floating potential profiles has a radial extension of about 1 cm. There is a strong radial variation in the floating potential just outside the flattening region. Good agreement was found between plasma profiles measured in a single plasma discharge,

as the probe system moves 10 cm into the plasma edge in about 100 ms, and plasma profiles measured shot by shot. The plasma potential has been estimated from measurements of the floating potential and the electron temperature using swept Langmuir probe methods. This shot to shot reproducibility in the plasma profile measurements is consistent with the static nature of the 8/5 island in the TJ-II stellarator.

These results can be interpreted as an increase of the sheared  $E \times B$  flow linked to the radial location of the 8/5 rational surface with a resulting radial gradient  $(dE_r/dr)B^{-1}$  of about  $10^5 \text{ s}^{-1}$ . Because the plasma edge radial and poloidal correlations are of the same order and TJ-II is a low magnetic shear stellarator, this can be considered to be a rough estimate of the shear decorrelation rate. This value turns out to be comparable to the inverse time of fluctuations measured in the plasma boundary in TJ-II. This result suggest the possible role of  $E \times B$  sheared flows linked to rational surfaces to explain the formation of transport barriers.

Preliminary measurements of broadband turbulence in TJ-II have shown that density fluctuation levels are in the range 10–30% with correlation times of (5–20)  $\mu\text{s}$  in proximity of the last closed flux surface.

Measurements with high spatial resolution have shown experimental evidence of confinement of non-thermal electrons (60 keV) linked to low order rational surfaces. The X ray flux (20–200 keV) signal indicates that those electrons are still confined near rational surfaces after the plasma shut down. This result can be interpreted as experimental evidence in favor of the existence of alternating conduction layers in magnetically confined plasmas linked to low order rational values.

Understanding the mechanisms which drive  $E \times B$  sheared flows linked to rational surfaces is an important physics issue in tokamaks and stellarator devices. Different mechanisms should be considered for the generation of  $E \times B$  flows at resonant surfaces. For instance,  $E \times B$  flows can be driven by the ion-electron flux difference created in the vicinity of rational surfaces. The  $E \times B$  sheared flows linked to the radial location of rational surfaces could also be explained by taking into account the rational surface induced anisotropy in the structure of turbulence. Radially varying non-isotropic turbulence allows fluctuations to

re-arrange the profile of poloidal momentum, thereby generating sheared poloidal flows [4].

High spatial resolution Thomson scattering measurements have revealed the presence of a fine structure in both density and temperature profiles. No consistent explanation exist at the moment to explain this observation but their possible link to the iota profile (i.e., rational surfaces) and the influence of plasma parameters (collisionality, magnetic well) is being investigated at present.

## 7. MHD Activity and Transport Analysis

Large ELM-like activity has been recently observed in TJ-II. The plasma develops bursts of magnetic activity (observed in the Mirnov coils signal), followed by a large and distinct spike in the  $H_\alpha$  signal. An increase of the electrostatic and magnetic fluctuations at the plasma edge and a cold pulse towards the plasma center are also characteristics of these events. The electron temperature measured by the Electron Cyclotron Emission system shows a pivot point at the plasma radius  $r_{\text{eff}} = 0.6$ . As a consequence, the electron temperature profile flattens at the plasma radius where the temperature is in the range of (100–200) eV. This flattening is explained in terms of an electron heat conductivity enhancement by a factor of two. Between ELM like events, the electromagnetic turbulence at the edge is reduced and the  $T_e$  profiles recovered. These phenomena are similar to ELM like events observed in other stellarators. For TJ-II plasmas with glow discharge in Ar, short (20 ms) but clear transitions to a high confinement regime, shown by transport analysis, has been found.

## References

- [1] C. Alejalde *et al.*, *Fus. Techn.* **17**, 131 (1990).
- [2] E. Ascasibar *et al.*, *J. Plasma Fusion Res. series 1*, 183 (1998).
- [3] M.A. Pedrosa, C. Hidalgo, B.A. Carreras *et al.*, in *Proceedings of the 25<sup>th</sup> European Conference on Controlled Fusion and Plasma Physics*, (European Physical Society, Geneva, 1999), P1.068.
- [4] M.A. Pedrosa, C. Hidalgo, B.A. Carreras *et al.*, in *Proceedings of the 25<sup>th</sup> European Conference on Controlled Fusion and Plasma Physics*, (European Physical Society, Geneva, 1999), P1.068.